# *Ex Vivo* Model of Biopsy Clip Migration in Breast Cancer

By:
Alysha Akhtar, Lucy Brown, Carly Nerger

University of Virginia, Biomedical Engineering
Spring 2025

Faculty Advisors:
Dr. Timothy Allen, UVA School of Engineering and Applied Science, Department of Biomedical Engineering
Dr. William Guilford, UVA School of Engineering and Applied Science, Department of Biomedical Engineering
Dr. Lynn Dengel, UVA School of Medicine, Department of Surgical Oncology

Word Count: 3101
Number of Figures: 7
Number of Tables: 0
Number of Equations: 1
Number of Supplements: 8
Number of References: 16

Approved: _____ Date: May 6, 2025

# *Ex Vivo* Model of Biopsy Clip Migration in Breast Cancer

**Abstract**

When a patient undergoes a mammogram, if there is a spot on the image that looks suspicious, a small sample is removed and sent for a biopsy and a clip is left in its place. These clips serve two purposes. If the biopsy is negative, they act as a future reference for physicians. If the tissue is abnormal, they serve as a marker for tumor removal. Currently, the two main options for biopsy clips are titanium clips that require a secondary procedure in order to localize the tumor during surgery or the HydroMARK™, a hydrogel-surrounded clip that can be localized in the operating room using ultrasound. The HydroMARK™ tends to migrate when the tissue decompresses, which reduces surgical accuracy and worsens lumpectomy margins. Currently, there is no method to measure this clip migration. Using bovine udder tissue as an *ex vivo* model, this study aims to develop a method of measuring clip migration and establishing a negative control. To replicate a mammogram, multiple iterations of a compression device were developed before settling on a triangular plate design with micrometer heads to allow for balanced and precise displacement. In lieu of commercially available biopsy clips, 26G wire and 34G wire were used to develop pin and coil clips, respectively. Images were taken in the xy- and xz-planes before and after tissue decompression and ImageJ was used to calculate clip displacement in 3D space. There was no significant difference in migration between the pin and coil clips ($p = 0.73$) and no significant difference in migration between mammary and fat tissue ($p = 0.37$). Ultimately, a negative control was successfully established because the average migration of titanium clips was less than the 5 mm threshold for clinically harmful migration.

Keywords: biopsy, breast cancer, clip migration, lumpectomy

---

**Introduction**

For a disease as common as breast cancer, with 1 in 8 women in the U.S. being diagnosed during their lifetime, the clinical protocols for diagnosis and treatment are incredibly inefficient (1). One notable example of an inefficient clinical protocol is the lumpectomy—a surgical treatment for breast cancer during which the surgeon excises the cancerous tissue but leaves the healthy breast intact. There are two main issues with this clinical workflow: procedural inefficiency and imperfect outcomes.

The procedural inefficiency at play here is due to the long clinical pathway that patients with non-palpable breast tumors must go through before their lumpectomy. Starting at age 40, women are encouraged to get mammograms every two years for screening (2). A mammogram consists of compressing the breast tissue between parallel plates and taking an X-ray image. If the image shows any tissue abnormalities, a followup biopsy is done under this same mammogram compression. These masses are non-palpable, so a biopsy clip is placed to allow for future localization of this lesion, either in the operation that follows or in future mammograms to note where a biopsy has previously been performed. If the biopsy shows that the mass is cancerous or growing rapidly enough to justify removal, a secondary localization procedure is required for the surgeon to locate the lesion during surgery. There are two common secondary procedures: the wire method and the radioactive seed method. The aptly named wire method is when a wire is inserted to mark the biopsy clip's location using mammography, protruding from the skin and taped in place. This allows the surgeon to follow the path of the wire to the lesion. This is typically done shortly before the operation, as it can be very uncomfortable for the patient and their movement is restricted by the wire (3,4). The second method, the seed method, is when a radioactive seed is inserted next to the biopsy clip. This allows the surgeon to locate the seed using a probe that detects radioactivity, pointing them in the direction of the seed and

thus the biopsy clip and tumor. However, this also is typically done shortly before an operation because radioactive material is not safe to remain in the body indefinitely (5).

This pathway is unnecessarily long and uncomfortable for the patient, and with the currently available technologies it cannot be improved. These secondary localization methods cannot be used during the initial biopsy because neither are compatible with staying in the body long term if surgery is not indicated. Additionally, the technology used to insert them to the location of the biopsy clip is not present in most operating rooms, so these procedures cannot be combined with the lumpectomy when the patient is under general anesthesia. However, because the wire and seed are both inserted under local anesthesia, they are incredibly uncomfortable for the patient. These localization procedures can occur anywhere from several days before the lumpectomy to the morning of, and this wait time increases the stress on the patient (6). Sometimes, the wire is left for a week after the procedure which increases the stress on the patient during the recovery process (7). Additionally, the extra procedure presents equity issues that can further exacerbate disparities in healthcare access. "Hidden costs of healthcare" like time off of work and travel expenses are amplified with each additional procedure, making it disproportionately difficult for patients of lower socioeconomic status to get proper treatment (8). With 170,000 lumpectomies performed annually in the U.S. (9), extra appointments significantly increase strain for hospitals in scheduling, staffing, and supplies, as well as increasing patient discomfort and risk of infection.

The second main issue in the clinical workflow leading to a lumpectomy is imperfect outcomes. There is an available technology that mitigates the previously mentioned issues in procedural inefficiency. The HydroMARK™ is a one-step biopsy clip that is intraoperatively visible and safe to remain in the body, but it introduces a new problem while solving the former. The HydroMARK™ is a biopsy clip surrounded by an expandable hydrogel, allowing the surgeon to locate the clip using ultrasound since the hydrogel is anechoic (10). Ultrasound technology is commonly available in the operating room, so this localization procedure can be done when the patient is under general anesthesia immediately before their lumpectomy. However, this clip has been shown to extrude or migrate after placement in 51.6% of patients (11). One study found that on average, the HydroMARK™ migrated 7.7 mm from the biopsy site (12). The clip is inserted when the breast is compressed during mammography, so the decompression of the tissue leads to its migration away from the original biopsy site. This reduces the effectiveness of the marker as a tumor localization method, which can result in poorer surgical margins and increase the likelihood of recurrence of the cancer. In fact, the migration of these clips are severe enough that they are not used in the UVA Health System. The surgeon needs to be confident that, when it is time to operate, the clip is exactly where it was placed, as the clip's location is a main determinant of what tissue is excised and what remains in the breast. These inaccuracies in biopsy site marking can have oncological consequences, if some of the cancerous cells are left behind, as well as cosmetic effects, if too much healthy tissue has to be removed in order to counteract this uncertainty. Additionally, in rare cases clips have been shown to migrate so drastically that they extrude from the skin (13), causing incredible pain for the patient as well as aesthetic complications.

Ultimately, a novel one-step biopsy clip that is intraoperatively visible but mitigates the migration seen with HydroMARK™ should be developed to streamline this clinical workflow. However, there is currently no effective method of measuring biopsy clip migration in a model system, so these clip technologies cannot be improved until they can be appropriately tested. Thus, the goal of this project was developing an effective *ex vivo* model system of biopsy clip migration in breast cancer. Our aim is to determine an appropriate tissue model to mimic human breast composition and a method for simulating the conditions under which biopsy clips migrate. The standard metal biopsy clips are known to be reliable markers, so we hypothesize that by compressing a model tissue, inserting metal biopsy clips, decompressing the tissue, and measuring clip displacement, we can establish a negative control system for biopsy clip migration.

## Results

*Modeling mammogram*

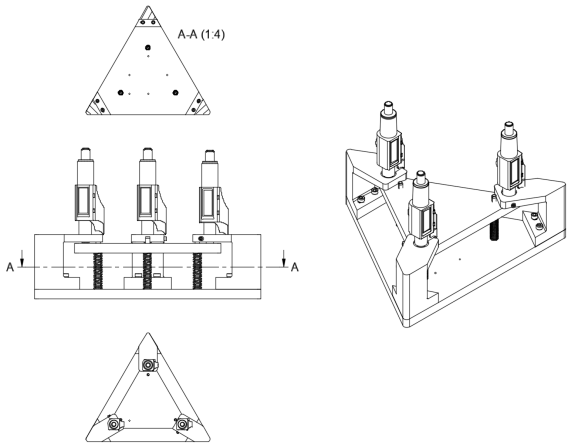


Figure 1. Final compression device assembly in CAD.

Figure 1 depicts the full compression device assembly. The device consists of 9 different parts: a large acrylic plate, a small acrylic plate, 3 micrometer head posts, 3 micrometer heads, 3 pins, 3 springs, 6 metal balls, 6 screws, and 3 set screws. The materials and dimensions of this device were determined in accordance with constraints and assumptions outlined in Materials & Methods. The larger acrylic plate serves as the bottom plate of the compression device and is an equilateral triangle with rounded edges. Embedded in this plate are 5 of the metal balls in a square pattern with one additional ball at the corner (visible under X-ray in Figure S1A). The smaller acrylic plate serves as the top plate of the compression device and is also an equilateral triangle with rounded edges. This plate also has a metal ball embedded in its surface, which sits directly above the ball in the bottom left corner of the bottom plate, defining the z-axis in the xz-plane images (Figure S1B). The two plates are separated by springs that sit around the corners of the triangle, right in front of where the micrometer head sits. These springs are held in place by pins that are connected to the bottom plate. The micrometer head posts are screwed into the top of the bottom plate, one on each corner. The micrometer heads sit in the hole on the overhang of the posts with the screen and rotational mechanism above it and the anvil below. The micrometer head is stabilized in the post by a set screw that goes into the side of the post, perpendicular to the micrometer head, and presses into the barrel.

The device is operated by sliding tissue between the two acrylic plates into the center of the triangle (Figure S2). Each micrometer head is turned clockwise, deploying the anvil and effectively pressing the top acrylic plate down and compressing the springs and the tissue. The micrometer head displays a value indicating the distance that the anvil is extended, allowing each one to be turned to a set distance. To decompress, each micrometer head is turned counterclockwise until the screen reads zero. As the anvil retracts into the micrometer head, the springs support the top acrylic plate, allowing it to return to its original position.

*Modeling migration*

Clips were deployed at the approximate center of the tissue using piercing needles, which were inserted along the y-axis. After X-ray images were captured for clips in compressed and decompressed tissue states and analyzed using ImageJ, the procedure for which is outlined in Materials & Methods, the migration distance for the various test groups was analyzed. The average migration distance was 0.2 ± 0.2 cm (mean ± sd) for the pin-shaped clips and 0.3 ± 0.1 cm for the coil-shaped clips (Figure 2). However, this difference was insignificant with a t-test p-value of 0.73.

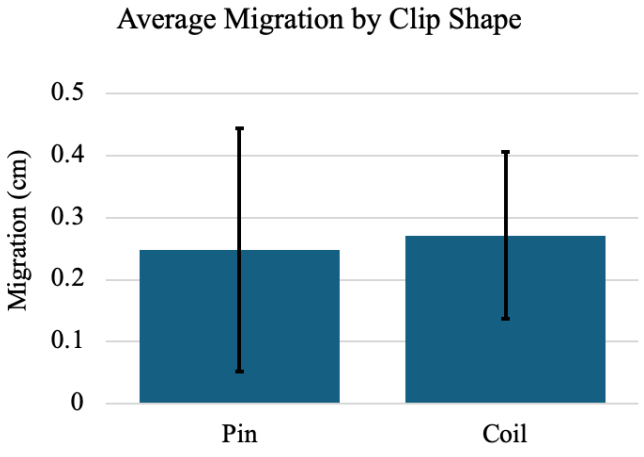


Figure 2. Average migration by clip shape. The difference in migration between pin (N = 6) and coil (N = 9) shaped clips was insignificant with a t-test p-value of 0.73. Error bars represent standard deviation.

Furthermore, the average migration distance was 0.3 ± 0.2 cm in mammary tissue and 0.3 ± 0.2 cm in fat

tissue (Figure 3). Once again, this difference was insignificant with a t-test p-value of 0.37.

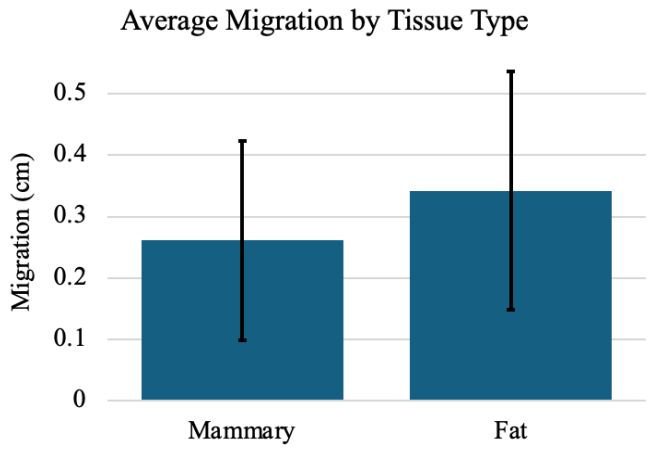


Figure 3. Average migration by tissue type. The difference in migration within mammary (N = 13) and fat (N = 2) tissue was insignificant with a t-test p-value of 0.37. Error bars represent standard deviation.

Based on clinical observations of lumpectomy procedures as well as insight from our clinical advisor, the threshold for clinically harmful migration that negatively impacts the ability to effectively remove a lesion was determined to be 5 mm. Thus, we considered the number of trials for each test group that demonstrated a harmful level of migration. One (1) of 6 trials using the pin-shaped clips and 1 out of 9 trials using the coil-shaped clips demonstrated a clinically harmful level of migration greater than the 5 mm threshold (Figure 4).

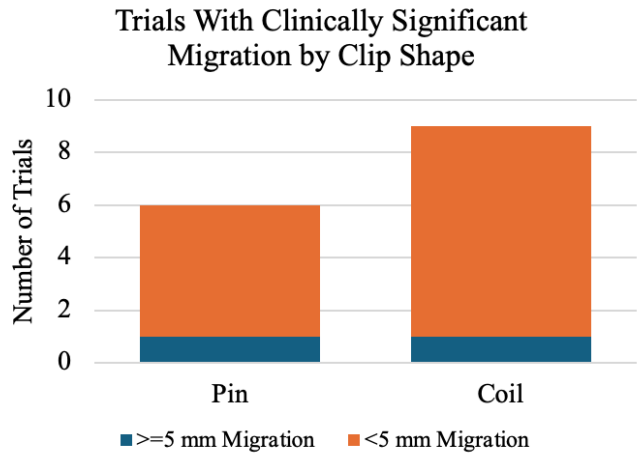


Figure 4. Count of trials with clinically significant migration distances by clip shape. Both clip types had 1 trial with clinically harmful migration.

Analyzing clinically harmful migration based on tissue type, it was determined that 2 out of 13 trials conducted within the mammary tissue had clinically significant levels of migration while 0 out of 2 trials conducted within the fat tissue had clinically significant migration (Figure 5).

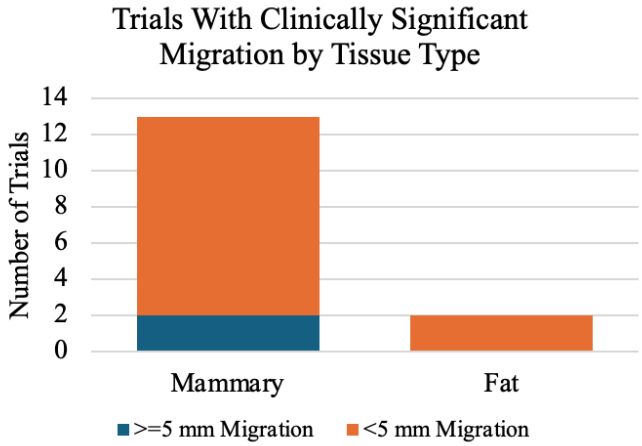


Figure 5. Count of trials with clinically significant migration distances by tissue type. 2 of 13 mammary tissue trials and 0 out of 2 fat tissue trials had clinically harmful migration.

Migration in the x-, y-, and z-dimensions was considered in addition to overall migration. The migration distance for each test group in each dimension can be visualized in Figure 6. Most of these migration distances indicate no dimensional trends in migration of titanium clips because the p-values from a one-sample t-test against 0 were greater than 0.05. However, for x-dimensional migration of coils in fat tissue and x-dimensional migration of pins in mammary tissue, the difference *was* significant, with a p-value less than 0.05.

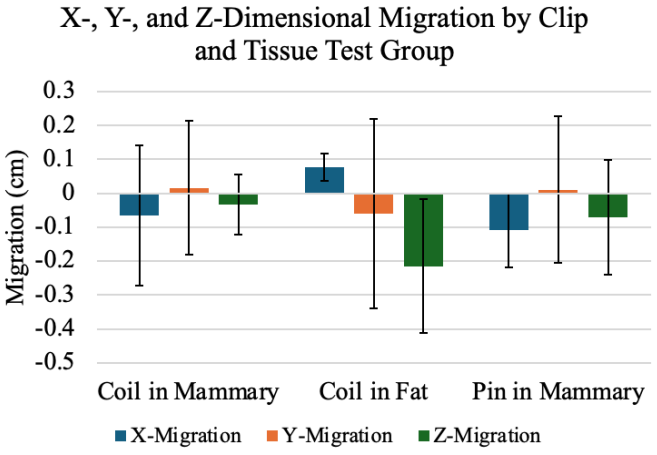

Figure 6. Migration distance in x-, y-, and z- dimensions by clip shape and tissue type test group. Test groups include coil in mammary (N = 7), coil in fat (N = 2), and pin in mammary (N = 6). The x-dimensional migration of coils in fat tissue and pins in mammary tissue was significant with one-sample t-test p-values less than 0.05. Error bars represent standard deviation.

**Discussion**

By measuring migration in titanium wire clips and demonstrating that this migration is clinically insignificant, we have successfully established a negative control for future testing to compare to HydroMARK™ clips, along with a model system that can be used to study HydroMARK™ migration. Our data show that the titanium biopsy clips migrated less than the 5 mm threshold for clinically harmful migration in all but two trials. The average migration indicates that movement of these clips is typically expected to be below 5 mm for all test groups. There was also no significant difference in migration between coil and pin clip shapes or between fat and mammary tissues, which indicates that the absence of clinically harmful migration is consistent for all titanium biopsy clips across test groups. In addition, based on the analysis of migration in the x-, y-, and z-dimensions, most of the test groups demonstrated no trends in direction of migration. This is understandable, since the magnitude of migration was determined to be insignificant. However, the x-dimensional migration for both coil clips in fat tissue and for pin clips in mammary tissue was determined to statistically differ from 0. Thus, further testing with a greater number of trials should be done to analyze the directionality of migration. Based on this initial analysis, we cannot clearly determine that significant migration happens in any specific direction. While the positioning of the tissue was not linked to any anatomical features, the lack of directional results indicates that the migration along the axis of compression, in this case the z-axis, or along the axis of insertion, in the case the y-axis, was not significant.

A major source of potential error is that two days passed between trials conducted with most of the pin and coil shaped clips, so tissue degradation could have occurred during this time and affected the results. In addition, although migration for each trial was analyzed twice by different team members, slight variations in measurements in ImageJ could have affected the results. During a few trials, the clip was not ejected from the piercing needle into the tissue so the insertion had to be redone, which could have affected the integrity of those tissue samples. There were also only two trials conducted using the fat tissue and no pin-shaped clips were inserted into fat tissue due to the difficulty of effectively inserting clips into this firmer tissue. However, based on our results, our compression device and measurement methods will help future work by providing an appropriate method for modeling and measuring clip migration.

A limitation of this project is that the HydroMARK™ clips were not used. We were unable to acquire HydroMARK™ clips from Mammotome. Future studies will ideally be able to purchase HydroMARK™ clips and thus measure their migration. Additionally, we were unable to acquire medical-grade biopsy clips and had to create our own. The appropriate wire was used and manipulated into the same shape as these medical-grade clips, but they were not the exact clips used in clinical settings.

The broader impact of our project is largely in its facilitation of future work that will directly improve clinical practice. By testing with HydroMARK™ clips in the future, the mechanisms of migration will hopefully be elucidated to inform next steps. Perhaps the clip migrates according to the angle of clip insertion, such that procedural modification would be sufficient to solve this clinical issue. It is also possible that there is no visible pattern in clip migration and the clip itself must be modified to improve its performance. Prototypes could alter the surface properties of the hydrogel or decrease its expansion time to increase the likelihood the clip will stay put during tissue decompression.

Furthermore, this project did not represent the biopsy cavity within the breast tissue. Rather than inserting clips directly into solid tissue, future work could excise a small portion of tissue representative of the tissue removed during a biopsy in order to reflect the condition of a biopsy cavity into which clips would actually be inserted. Once the migration of HydroMARK™ clips is understood in a more biologically relevant setting, future research can be conducted to determine how and why these clips migrate

and new designs can be developed to mitigate this migration.

Our work is a first step towards developing one-step biopsy clips that mitigate migration, which will enable future physicians to provide their patients with a more comfortable and streamlined process of localizing a tumor for a lumpectomy. Hundreds of thousands of patients per year (9) will spend less time in the clinic and experience less discomfort while costs associated with a lumpectomy will decrease for both hospitals and patients.

**Materials & Methods**

*Modeling breast tissue*

Human breasts and bovine udders are similar in composition and function (14,15). Both contain similar adipose tissue, mammary glands, and nipples. The glandular tissue was the primary interest as it is most similar to the fatty tissue of the human breast. One udder was obtained from a pregnant heifer and one was obtained from a non-pregnant heifer. These were provided to us by Mullins Slaughterhouse. The non-pregnant udder was composed of only fat and was not a fully developed udder. This tissue was used for preliminary tests to ensure our deployment method was sound. The pregnant udder had four separate glands, made up of glandular tissue, and each had a distinct teat. These were separated with a chef's knife and the glandular and fat tissue were separated. These were then cut into approximately 2 x 2 x 2 inch cubes. Due to the irregular shape of the udder, portions were not exact, but all cubes were almost entirely composed of mammary or fat tissue. Each cube was inserted into the center of the compression device along the y-axis.

*Design methodology*

In order to develop a device to compress tissue and mimic the conditions of biopsy clip insertion during a mammogram, we iterated through multiple designs. The basic structure that our design had to adhere to was two parallel plates that can be easily moved up and down by a known displacement for tissue compression. This device also needed to be compatible with the X-ray machine used for imaging, in regards to both size and materials. Thus, the parallel plates used to compress the tissue had to be radiolucent so that the tissue boundaries and clip location were visible. Additionally, radiopaque markers had to be incorporated to define a coordinate system that is clearly visible in X-ray images for measurement of displacement. However, this method of determining clip location is limited by the lack of precision inherent in manually measuring movement and defining the scale in our images, in comparison to some X-ray machines whose images are automatically calibrated to real distances.

Many alternative designs were considered before settling on our final design. Our first iteration of the compression device was very simple, consisting of two square plates with holes at each corner (Figure S3). Bolts would be inserted in these holes and nuts would be placed on the surface of the top plate, which could be turned with a wrench to compress the top plate downwards. We decided to use acrylic for the material of the parallel plates because it is transparent and radiolucent, allowing for visibility during clip insertion as well as in the X-ray images. To increase the precision of compression by allowing for measured displacement, we incorporated a micrometer head into the second iteration of our design. We proposed two square plates, where the bottom one had a post with an overhang containing a smaller plate attached to the bottom of a micrometer head anvil to allow for precise movements of the top plate (Figure S4). This design did not practically work with a micrometer head since micrometer heads push against the plate and are not designed to have attachments on the anvil.

We began to brainstorm designs that involved the micrometer head pushing against the plate to facilitate compression. For the third iteration of our device, we decided to incorporate triangular plates for increased stability and to ensure the plate remained flat during compression. This device had 3 pins with springs surrounding them, enabling the top plate to move up and down along the pins with the springs holding the plate up to return it to its decompressed location. Screws marked a coordinate plane on the top and bottom plates. There was a post for 3 micrometer heads on each corner, which included hinges to lift the micrometer heads up to make room for the top plate to be lifted and the tissue to be inserted (Figure S5).

*Modeling breast compression*

Our final design was quite similar to the third iteration of the design, but without the hinges and using small metal balls instead of screws to mark the coordinate axes. Additionally, we made small changes to ease the logistical process of assembling the device and increase its stability. These changes included using two screws instead of one to secure the micrometer head post to the bottom plate, and using a slot for one of these screw holes on the post to account for manufacturing error in the location of the holes on the bottom plate after they have been drilled and tapped.

The incorporation of a digital micrometer head for plate displacement introduced a new constraint to our design. A study showed that average non-compressed breast thickness is around 8.2 cm, and this was compressed during mammography to a new thickness of 5.4 or 4.7 cm (16). This is compression of slightly less than half the tissue thickness, so we chose 50% compression as the goal for our device to appropriately represent mammography. Thus, the tissue size we could use was constrained by the selection of digital micrometer heads available for purchase, since the maximum displacement of these devices was 25 mm. These design constraints assume that compressing a cube of tissue in the center of parallel plates is an acceptable representation of the compression during mammography, since the tissue in this case is isolated from the surrounding anatomical structures, such as the bones, skin, and muscles. We settled on a tissue size of 50 mm x 50 mm x 50 mm, so that the tissue is small enough for a 25 mm micrometer head to compress the tissue to 50% of its original height, but still large enough to exhibit migration.

The construction process for our compression device was split into three steps: 3D printing the micrometer head posts, laser cutting the acrylic plates, and assembly. In order to 3D print the posts for the micrometer heads, CAD designs were imported into Bambu studio for printing with the Bambu Lab X-1 Carbon printer. PLA Basic filament was used for the device, and Bambu support for PLA/PETG for the support filaments. These posts were designed with a 12.1 mm hole on the top face for the micrometer head to sit in. A 4 mm hole sits perpendicularly to this, in which a threaded insert for an M3 screw was melted. The micrometer head was inserted into its place and an M3 screw was secured against its side, allowing it to stay in place against the force on the top plate from the tissue being compressed. Additionally, the bottom support of this post contained a 5.2 mm diameter hole and slot for M5 screws to secure the post to the bottom plate. The fully dimensioned design of the post as printed is shown in Figure S6A.

Next, two 12 in x 12 in x ⅜ in acrylic plates were laser cut for the top and bottom compression plates. The top plate, fully dimensioned in Figure S6B, is an equilateral triangle with side lengths of 200 mm, with rounded corners of radius 5 mm. 40 mm from each vertex is a 5.302 mm hole, which was laser cut to fit the 7/32 in diameter split pins. The bottom plate, fully dimensioned in Figure S6C, is an equilateral triangle with side lengths of 305 mm, with rounded corners of radius 5 mm. At each corner, two 2 mm pilot holes were cut to define the location of the M5 screws. A 5/32 in drill press bit was used to drill out these holes, which were tapped with an M5 0.8 pitch tap. Three 5.302 mm holes sit directly below their counterparts on the top plate, extruding 7.5 mm into the plate for the pins to sit securely within the acrylic but not go entirely through it. Finally, the centerpoints of each side of a 50 mm square centered on the centerpoint of the plate were marked with 2 mm circles engraved onto the acrylic. The bottom left corner of this square was also engraved to mark the origin of our coordinate system, and this location was marked on the top plate as well. Shallow holes, about 1/16 in depth, were drilled at the center of these markings with a 1/16 in drill bit. A small roller bearing was broken apart using the arbor press, and the small metal balls inside were heated up with the soldering iron and inserted into the 1/16 in holes in order to mark the axes of a coordinate plane.

To assemble the device, the split pins were first inserted into the bottom plate using the arbor press to ensure they fit tightly for stability. Next, 2.5 in long springs with outer diameter 0.3 in and spring rate 1.1 lbs/in was placed surrounding the pins. The pin holes in the top plate were expanded using a ¼ in drill bit to ensure the top plate could rest on the spring while still moving freely on the vertical axis around the pins. The micrometer head posts were then secured to the bottom plate using M5 screws.

*Modeling migration*

To make pin clips, 26G wire was cut to 1 cm and folded in half at the 5 mm mark. The coil clips were constructed using 34G wire wrapped around a 16G needle and trimmed at each end.

To deploy clips within tissue, two different gauges of hollow, beveled piercing needles were purchased: a 12G needle and a 14G needle. A clip was placed into the hole of the 12G needle. The 12G needle was used to pierce into the tissue so that the sharp end of the needle was located at the desired clip insertion site. Then, the 14G needle was inserted through the hole of the 12G needle from the flat back end in order to push the clip completely through the needle and into the tissue. Initially, we encountered the issue of the clip getting lodged into the hole of the thinner needle. In order to remedy this, hot glue was used to enclose the holes on either end of the 14G needle to prevent clips from getting stuck within the needle so that they could be effectively pushed out into the tissue.

At Fontaine Research Park, a Siemens Arcadis Varic C-Arm X-ray imaging machine was used to image clip location within the tissue in compressed and decompressed states. In order to simulate clip deployment during a mammogram, a piece of tissue was inserted between the plates of the compression device. Then, the micrometer heads were used to precisely lower the top plate and compress the piece of tissue by 25 mm from its original 50 mm height to a compressed height of 25 mm. Once the tissue was compressed, a clip was placed into the 12G needle and inserted into the approximate center of the tissue, at an angle perpendicular to the x-axis. Then, the 14G needle was used to push the clip through the outer needle and into the tissue. The X-ray machine was used to take images from the top of the device to capture the clip's location in the xy-plane. Then, the lever arm of the X-ray machine was rotated 90° to capture the location of the clip in the z-dimension. To decompress the tissue, the micrometer heads were reset to raise the top plate back up by 25 mm. X-ray images were once again taken from the same angles, capturing the xy-plane and the xz-plane. This process was completed for 7 coil clips within mammary tissue, 6 pin clips within mammary tissue, and 2 coil clips within fat tissue.

*Calculating migration*

Image analysis for migration calculation was done in ImageJ. Migration was conceptualized as the distance between the true final clip location ($x_f$ ,$y_f$ ,$z_f$) and the hypothetical ideal clip location post decompression ($x_i$',$y_i$',$z_i$') had it not moved within the tissue relative to its original location under tissue compression ($x_i$ ,$y_i$ ,$z_i$), shown in Figure 7. Meaning, if the clip was precisely in the center of the compressed tissue with regard to length, depth, and height, ($x_i$',$y_i$',$z_i$') would be a point directly in the center of the decompressed tissue, taking into account changes in overall tissue dimensions with the removal of compression pressure. In order to calculate this displacement, clip location first had to be established in a three-dimensional coordinate system. The location of the small metal balls within the compression device established this coordinate system, allowing for measurement of the precise location of clips in the compressed and decompressed X-ray images so that the migration of clips between these states could be calculated. Measured distances on the compression device were used to calibrate ImageJ for the relationship between pixels and real distance. For the xy-plane, this was the distance between the metal ball defining (0,0) and the other metal ball on the x-axis. For the xz-plane, measurements between the metal balls on the top and bottom plates were taken for micrometer heads set to 0 mm and 25 mm for decompressed and compressed states, respectively.

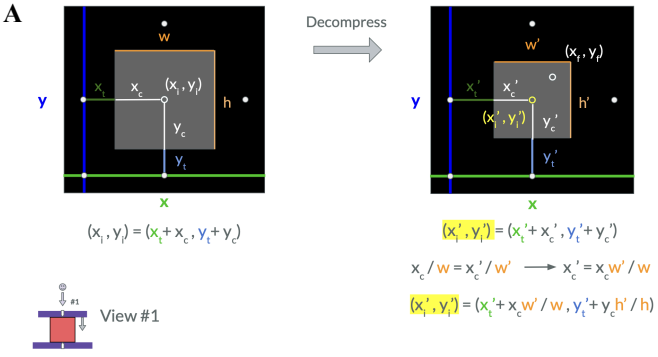

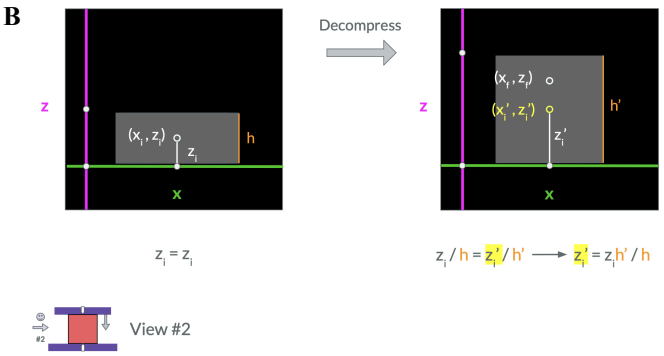


Figure 7. Calculation of clip displacement upon tissue decompression in xy- (A) and xz- (B) planes.

Calculations began with the xy-plane in order to define ($x_i$ ,$y_i$), shown in Figure 7A. Compressed tissue height *h* and width *w* were calculated as an average of 5 line segments drawn across the tissue (Figure S7). $x_c$ and $y_c$ represent the depth of the clip within the tissue in the x- and y-directions, measured starting at the tissue boundary along a line segment perpendicular to each axis. Decompressed height *h'* and width *w'* were measured using the same standards as for compressed tissue. To define the hypothetical ideal clip location post-migration ($x_i$',$y_i$'), a simple ratio was established to compare the compressed tissue width *w* to $x_c$ and the decompressed tissue width *w'* to the (not yet established) clip location within the decompressed tissue $x_c$'. The same ratio was established in y with corresponding heights. Thus, ($x_i$',$y_i$') was determined to be equal to ($x_t$'+ $x_c$w' / w , $y_t$'+ $y_c$h' / h). A similar analysis was performed on the xz-plane images to quantify the location of the clip in the z-plane $z_i$' had it not migrated (Figure 7B). Final clip displacement in three dimensions *d*, calculated using Equation 1, quantified the extent of clip migration upon tissue decompression. This analysis was repeated for all trials.

$$d = \sqrt{(x_f - x_i')^2 + (y_f - y_i')^2 + (z_f - z_i')^2}$$

Equation 1. Clip displacement in 3D space.

The values of *d* were averaged over all trials with the pin and coil clips, as well as for fat and mammary tissue in order to compare clip and tissue types (Table S1).

**Supplementary Material**

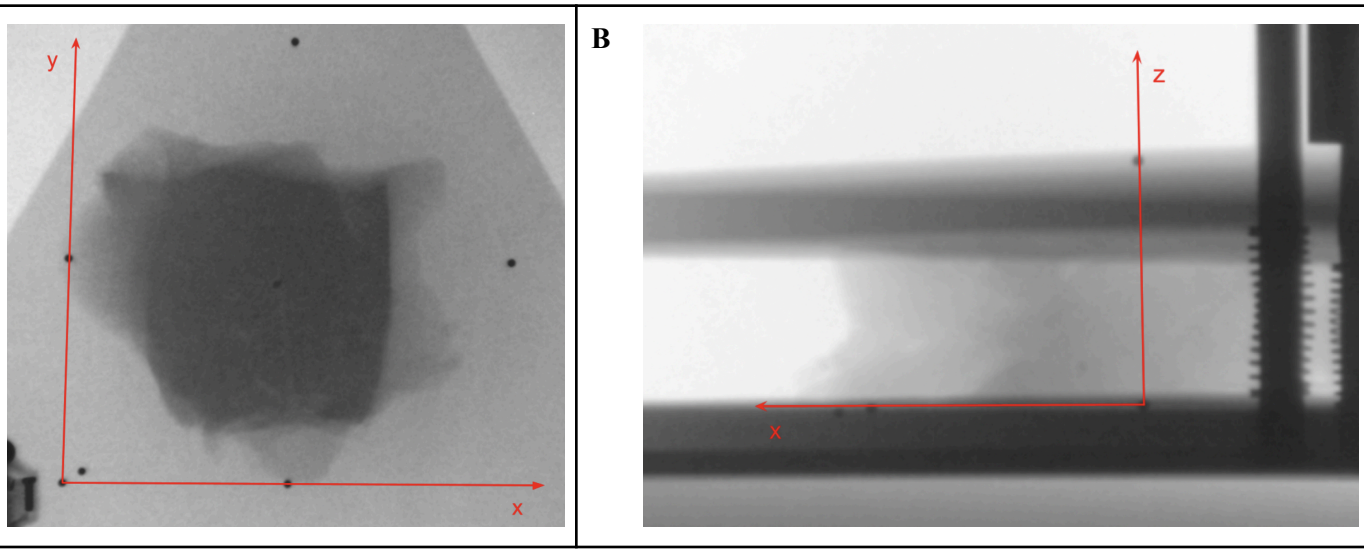


**Figure S1: Visualization of metal balls to define axes of coordinate plane under X-ray**. **1A:** Xy-plane. **1B:** Xz-plane.

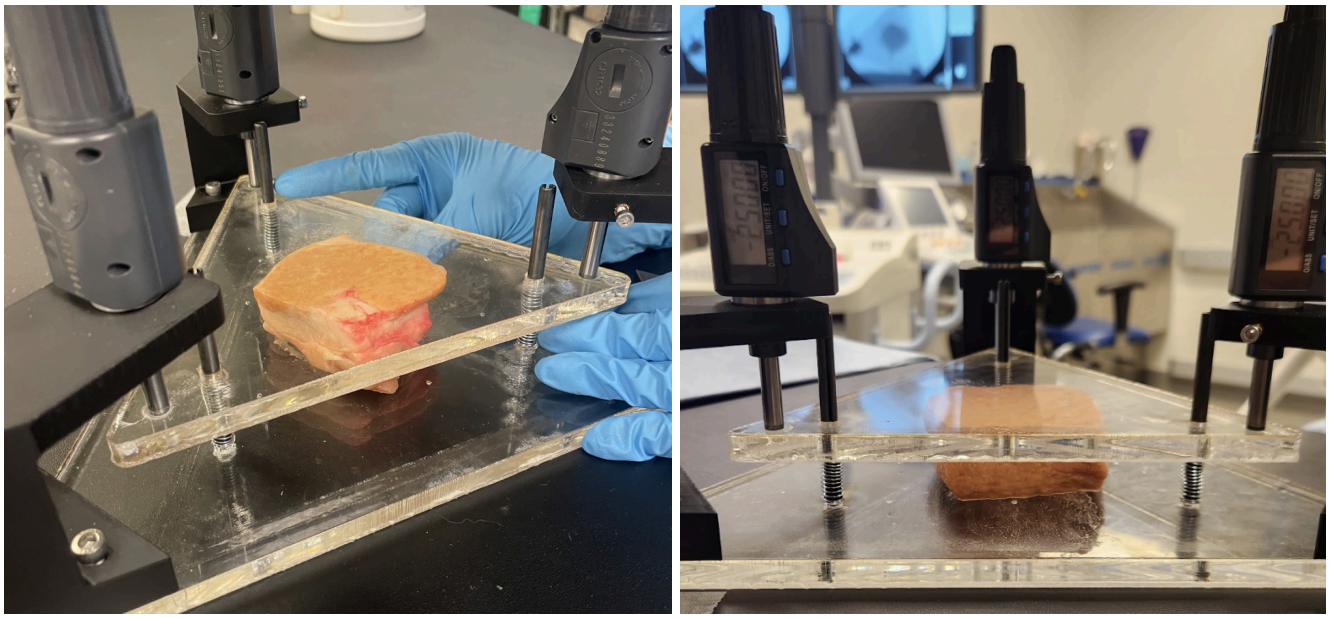

**Figure S2: Tissue placement within compression device.**

**A**

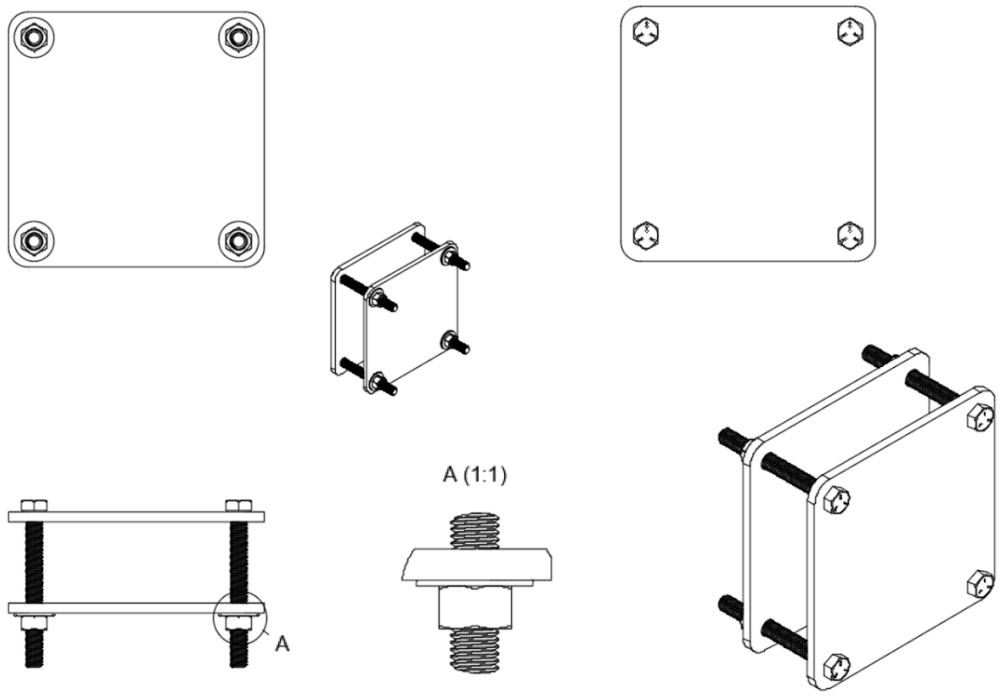


**B**

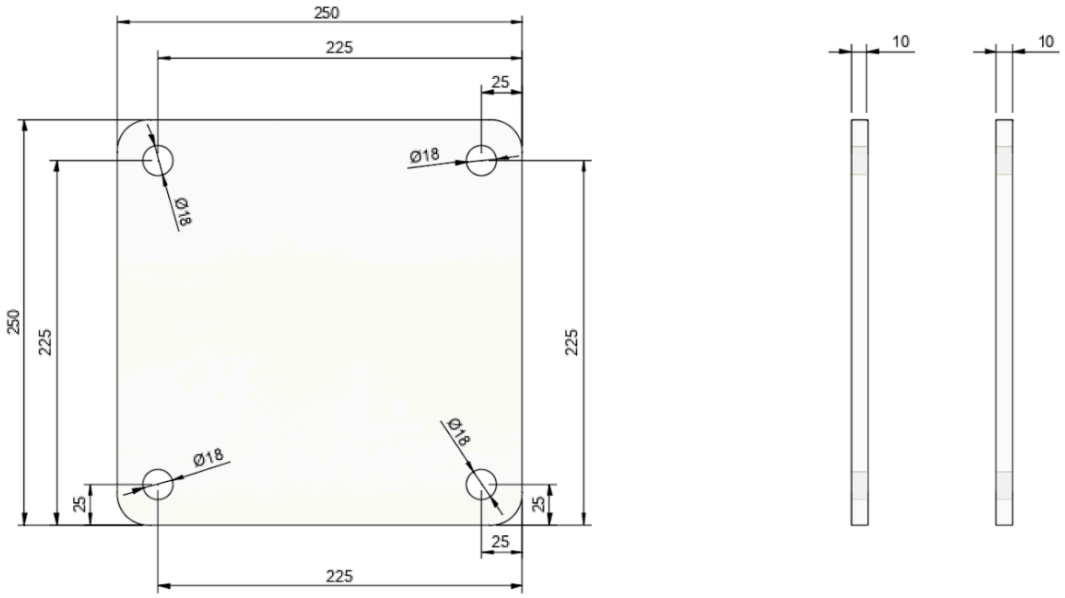


**Figure S3: Engineering design drawings of compression device iteration 1. 3A:** Overall drawing showing multiple perspectives of the assembled device, including nuts, bolts, and washers. **3B:** Engineering design drawing of the plates only, dimensioned for use with 3D printing or laser cutting.

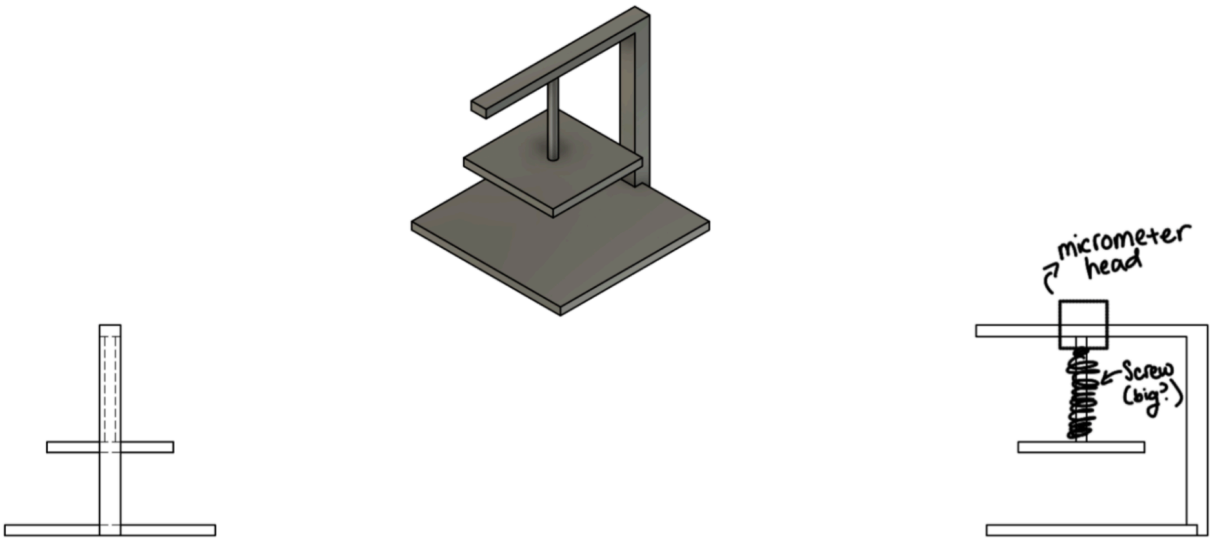


**Figure S4: Engineering design drawings of compression device iteration. 2** Rough sketch of how a micrometer head could be incorporated into preliminary compression design, including a micrometer head directly on top of a screw. This is based on a flawed understanding of a micrometer head's implementation and was quickly discarded.

**A**

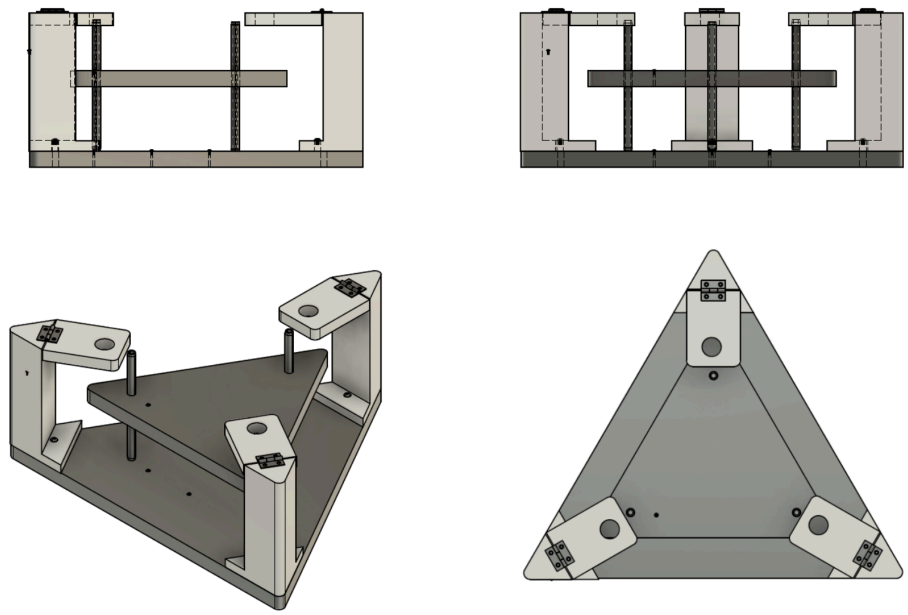

**B**

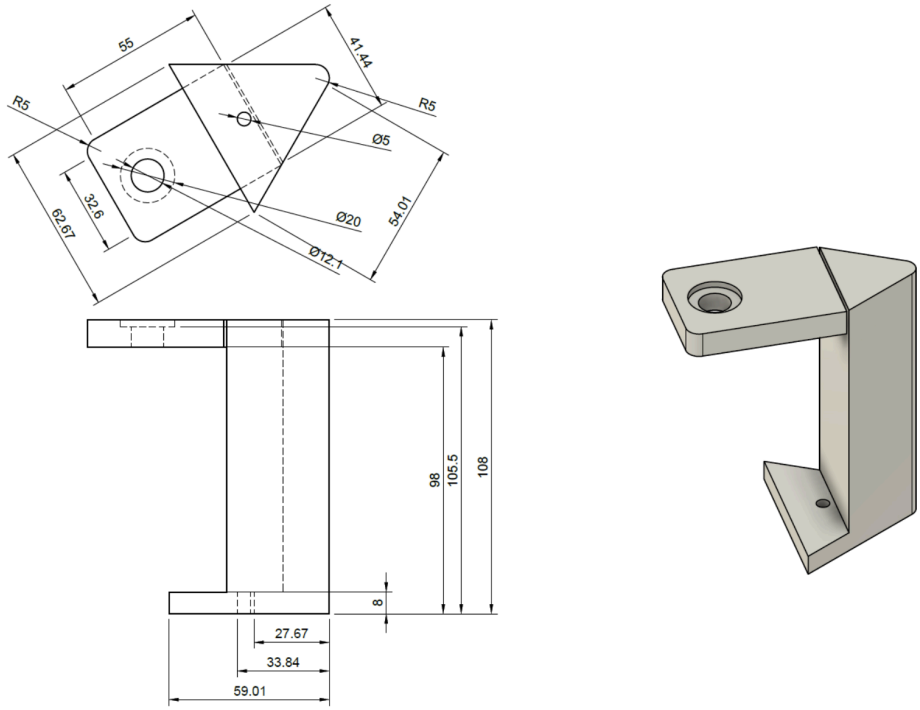


**Figure S5: Engineering design drawings of compression device iteration 3. 5A:** Overview of fully assembled compression device incorporating a hinge on the post (springs and micrometer heads not shown) **5B:** Dimensioned posts to support micrometer heads.

**A**

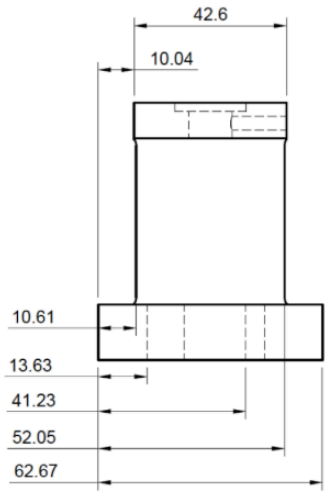
42.6
10.04
10.61
13.63
41.23
52.05
62.67

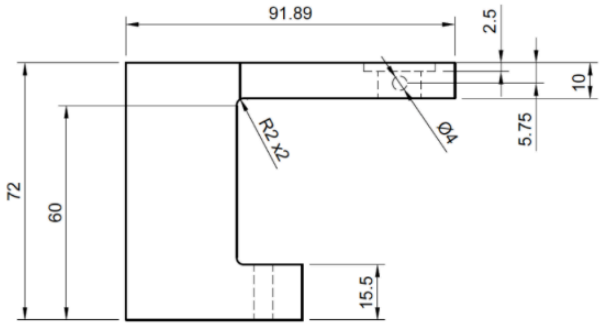
91.89
2.5
10
5.75
Ø4
R2 x2
72
60
15.5

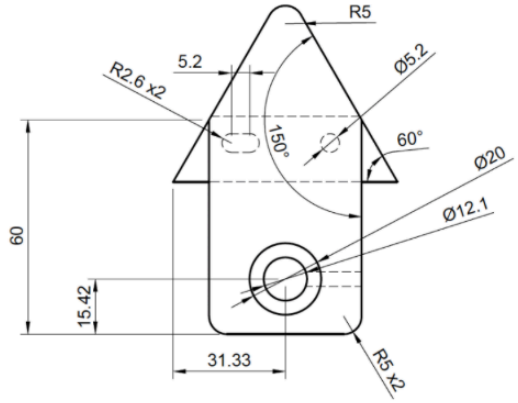
R5
5.2
R2.6 x2
Ø5.2
150°
60°
Ø20
Ø12.1
60
15.42
31.33
R5 x2

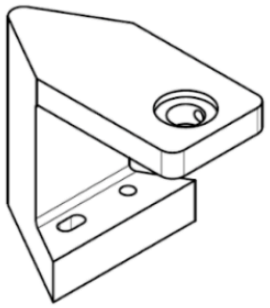

**B**

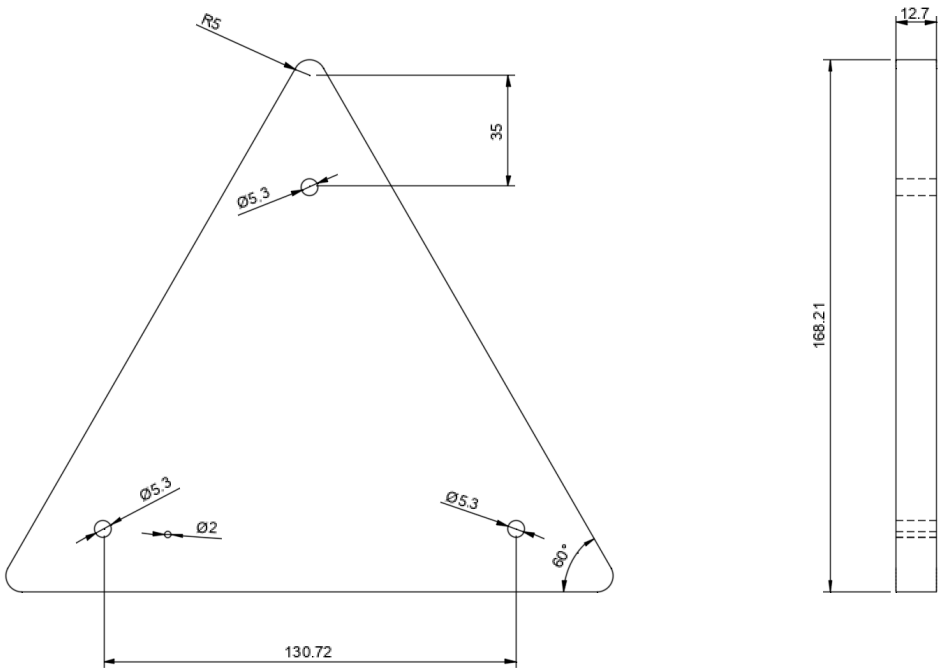


**C**

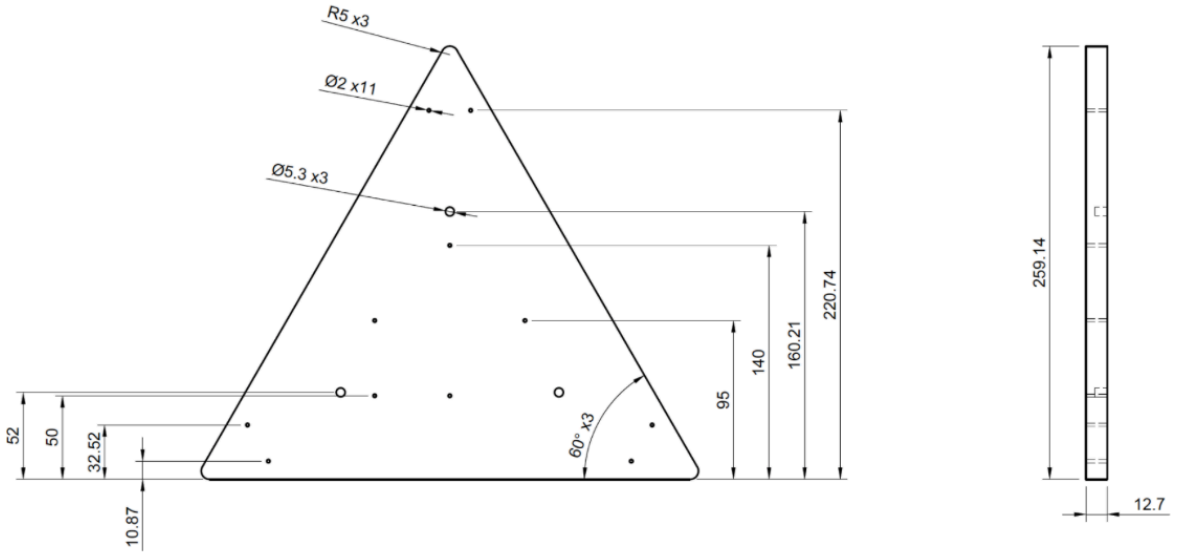


**Figure S6: Fully dimensioned engineering design drawings of 3D printed and laser cut compression device components in CAD. 6A:** Engineering design drawing of one of three posts for micrometer heads for 3D printing. **6B:** Engineering design drawing of top compressive plate for laser cutting in acrylic. **6C:** Engineering design drawings of bottom base plate for laser cutting in acrylic.

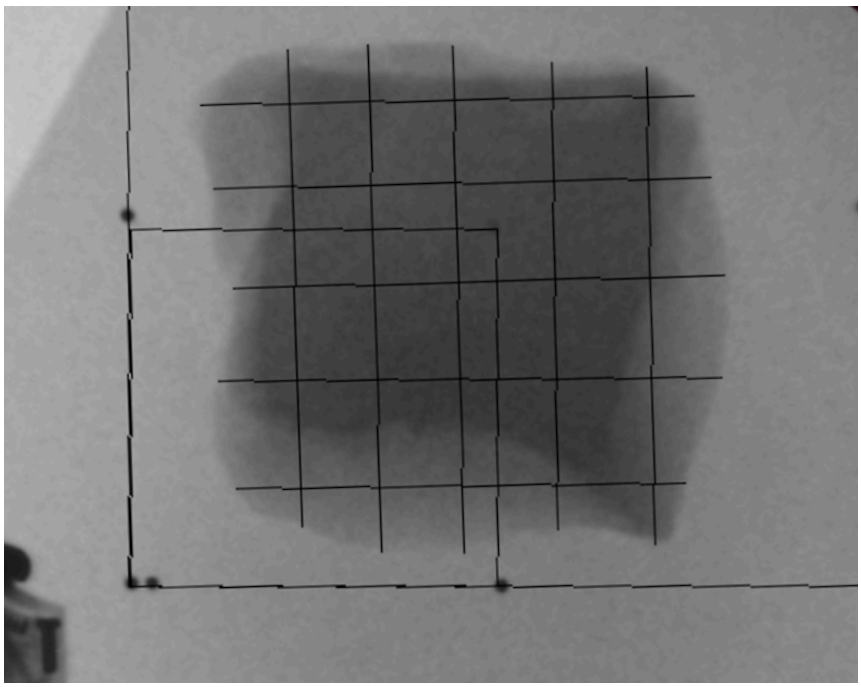

**Figure S7: Width and height measurements on real tissue shapes.**

**Table S1: Displacement measurements for mammary tissue.** Data reported as the average of two team members measurements.

| **Clip type** | $\mathbf{x}_{\text{displacement}}$ | $\mathbf{y}_{\text{displacement}}$ | $\mathbf{z}_{\text{displacement}}$ | $\mathbf{d}_{\text{overall}}$ |
|---|---|---|---|---|
| Coil | 0.000 | -0.135 | 0.000 | 0.151 |
| | 0.110 | -0.143 | -0.160 | 0.251 |
| | 0.076 | 0.173 | 0.072 | 0.245 |
| | -0.072 | 0.324 | -0.057 | 0.338 |
| | 0.072 | -0.169 | -0.085 | 0.205 |
| | -0.505 | 0.038 | -0.099 | 0.540 |
| | -0.172 | 0.097 | 0.078 | 0.224 |
| Pin | -0.010 | -0.012 | 0.007 | 0.048 |
| | -0.283 | -0.334 | -0.412 | 0.604 |
| | -0.145 | -0.124 | 0.095 | 0.220 |
| | -0.036 | 0.057 | 0.000 | 0.090 |
| | -0.086 | 0.213 | -0.036 | 0.236 |
| | -0.098 | 0.264 | -0.070 | 0.292 |

**References**


1. American Cancer Society [Internet]. 2025 [cited 2025 May 4]. Key Statistics for Breast Cancer. Available from: https://www.cancer.org/cancer/types/breast-cancer/about/how-common-is-breast-cancer.html

2. ACS Breast Cancer Screening Guidelines | American Cancer Society [Internet]. [cited 2024 Nov 15]. Available from: https://www.cancer.org/cancer/types/breast-cancer/screening-tests-and-early-detection/american-cancer-society-recommendations-for-the-early-detection-of-breast-cancer.html

3. Staff DF. Seed vs. Wire Localization: Lumpectomies for Breast Cancer [Internet]. Dana-Farber Cancer Institute. 2017 [cited 2024 Nov 15]. Available from: https://blog.dana-farber.org/insight/2017/07/patients-benefit-from-new-technique-in-lumpectomy-for-breast-cancer/

4. What Should I Expect During A Breast Biopsy? | Dr Garvit [Internet]. 2022 [cited 2024 Nov 15]. Available from: https://drgarvitchitkara.com/blogs/what-should-i-expect-during-a-breast-biopsy/

5. Radiation and health [Internet]. [cited 2024 Nov 15]. Available from: https://www.who.int/news-room/questions-and-answers/item/radiation-and-health

6. Mayo Clinic [Internet]. 2025 [cited 2025 May 5]. Lumpectomy. Available from: https://www.mayoclinic.org/tests-procedures/lumpectomy/about/pac-20394650

7. Needle Localization [Internet]. Dr. Jay R Anam. [cited 2025 May 5]. Available from: https://drjayanam.com/needle-localization/

8. Wheeler SB, Reeder‐Hayes KE, Carey LA. Disparities in Breast Cancer Treatment and Outcomes: Biological, Social, and Health System Determinants and Opportunities for Research. The Oncologist. 2013 Sep 1;18(9):986–93.

9. Rao R. The Cancer Letter. 2019 [cited 2025 Feb 11]. Reducing re-excisions How intraoperative 3-D specimen tomosynthesis ensures fewer repeat breast cancer surgeries. Available from: https://cancerletter.com/trials-and-tribulations/20190927_5/

10. HydroMARK Breast Biopsy Site Marker [Internet]. Devicor Medical Products, Inc; 2022. Available from: https://www.mammotome.com/assets/2022/06/hydromark-tri-fold-mdm-200565.pdf

11. Klein RL, Mook JA, Euhus DM, Rao R, Wynn RT, Eastman AB, et al. Evaluation of a hydrogel based breast biopsy marker (HydroMARK®) as an alternative to wire and radioactive seed localization for non-palpable breast lesions. J Surg Oncol. 2012;105(6):591–4.

12. Pinkney DM, Mychajlowycz M, Shah BA. A prospective comparative study to evaluate the displacement of four commercially available breast biopsy markers. Br J Radiol. 89(1065):20160149.

13. Ang BW, Lee YS, Lim GH. An unusual site for breast clip migration: A case report. Radiol Case Rep. 2023 May 12;18(7):2487.

14. Jaswal S, Jena MK, Anand V, Jaswal A, Kancharla S, Kolli P, et al. Critical Review on Physiological and Molecular Features during Bovine Mammary Gland Development: Recent Advances. Cells. 2022 Oct 21;11(20):3325.

15. Hovey RC, McFadden TB, Akers RM. Regulation of mammary gland growth and morphogenesis by the mammary fat pad: a species comparison. J Mammary Gland Biol Neoplasia. 1999 Jan;4(1):53–68.

16. Feder K, Grunert JH. Is Individualizing Breast Compression during Mammography useful? – Investigations of pain indications during mammography relating to compression force and surface area of the compressed breast. RöFo - Fortschritte Auf Dem Geb Röntgenstrahlen Bildgeb Verfahr. 2016 Dec 21;189:39–48.